Anisotropy of ^{39}K binding in C_8K studied by nuclear resonance photon scattering

R. Moreh
Nuclear Physics Laboratory, Department of Physics, University of Illinois at Urbana-Champaign, Champaign, Illinois 61820
and Nuclear Research Centre—Negev, P.O. Box 9001, 84 190 Beer-Sheva, Israel
and Department of Physics, Ben-Gurion University of the Negev, P.O. Box 653, 84 120 Beer-Sheva, Israel

W. C. Sellyey and D. C. Sutton
Nuclear Physics Laboratory, Department of Physics, University of Illinois at Urbana-Champaign, Champaign, Illinois 61820

H. Zabel
Department of Physics and Materials Research Laboratory, University of Illinois at Urbana-Champaign, Urbana, Illinois 61801
(Received 30 June 1986)

A new technique employing nuclear resonance photon scattering of bremsstrahlung has been used for studying the anisotropic binding of K atoms in the first-stage intercalated compound C_8K. The bremsstrahlung was obtained using an electron beam with $E_e = 8.5$ MeV. The scattered intensities from the 5.262- and 6.334-MeV levels in ^{39}K and from the 4.439-MeV level in ^{12}C were found to be dependent on the c-axis orientation of C_8K with respect to the photon beam in a nuclear self-absorption measurement. This behavior is interpreted in terms of the anisotropy in the Doppler broadenings of the ^{39}K and ^{12}C nuclear levels caused by the zero-point energies of the C_8K vibrational modes along and perpendicular to the graphite basal planes. The measured anisotropy was found to be somewhat higher than that calculated from the known vibrational spectra in C_8K.

I. INTRODUCTION

Graphite intercalation compounds are synthetic layered materials with pronounced anisotropic binding forces parallel and perpendicular to the intercalate planes. The anisotropy is expressed in the elastic, vibrational, and electronic properties and varies with the stage n of the compound, where the index n indicates the number of graphite planes between any successive intercalate planes. In this paper a nuclear resonance photon scattering (NRPS) experiment on stage-1 C_8K is discussed, which probes the anisotropy of the vibrational energies in and out of the intercalate plane by comparing the Doppler broadening of nuclear resonance levels in intercalated ^{39}K to those of an isotropic nuclear absorber. From the present NRPS experiment, effective temperatures $T_{\parallel}$ and $T_{\perp}$ can be evaluated, which are proportional to the mean-square velocities $\langle v^2 \rangle$ of the nucleus in question and can be related to Debye temperatures $\Theta_{\parallel}$ and $\Theta_{\perp}$, respectively. This method must therefore be distinguished from x-ray and Mössbauer measurements where the Debye temperatures Θ obtained are proportional to the mean-square displacements $\langle r^2 \rangle$ which are derived from the Debye-Waller factor. Thus the NRPS method effectively weights more strongly the high-frequency phonon modes, while the Debye-Waller factor measurements are more sensitive to the low-frequency modes. In this respect the NRPS technique can be viewed as a complementary tool to the conventional techniques. Another distinctive feature of the present method is that it enables one to study the vibrational frequencies of each component of the intercalation compound, namely, the C and K atoms separately. It should also be added that the NRPS method is fundamentally different from the Mössbauer effect because the widths of the nuclear levels in question at an excitation $E_x \sim 6$ MeV are around 0.01 to 1 eV, the Doppler widths are around ~ 8 eV for ^{39}K and $T = 300$ K, and the recoil energy $R = E^2/2Mc^2$ is ~ 500 eV which is much larger than the lattice binding in a crystal at $T = 300$ K. Hence, free recoil of the emitting or absorbing nuclei should always be assumed and no recoilless emission can possibly occur. The adequacy of the present technique for studying anisotropic systems was first illustrated in pyrolytic BN, where the photon resonance scattering from ^{11}B was measured. It was noted that the anisotropically scattered intensities were caused by different Doppler widths,

$$\Delta_r = E_\gamma (2kT_r/Mc^2)^{1/2} ,$$

of the nuclear levels,[1,2] indicating different effective temperatures T_r in the two perpendicular directions.

Since graphite intercalation compounds are highly anisotropic systems,[3,4] they are most suited for applying the present NRPS method. The suitability is in fact determined by two conditions.

(i) The scattered signal should be large, namely, $g\Gamma_0^2/\Gamma \approx 1$ eV, where $g = (2J+1)/(2J_0+1)$ is a statistical factor; J and J_0 are the spins of the excited and ground states of the scattering nucleus. Γ_0 and Γ are the ground-state width and the total radiative width of the nuclear level.

(ii) The Doppler width should be much larger than the level width, namely, $\Delta_r \gg \Gamma$.

These two conditions are met in intercalated compounds containing light nuclei with large values of Γ_0. In such compounds, the scattering intensity is sensitive to the orientation of the sample relative to the photon beam and

hence to the directional properties of the lattice dynamics of the system. Moreover, since the phonon spectrum of C_8K was studied in detail[5,6] it is therefore a relatively simple problem to calculate the effective temperature and to compare the results with the present measurement. It should be remarked that a different version of the present technique employing monoenergetic photon beams generated from the (n,γ) reaction has been used for studying the molecular orientation of the intercalant molecules in graphite intercalation compounds;[7] it was also used to study the orientation of adsorbed molecules with respect to the absorbing planes of graphite.[8] Because of the importance to understand various potentialities of the NRPS method, we will discuss it in some more detail below.

II. NRPS TECHNIQUE

The NRPS technique used here is illustrated in Fig. 1, which depicts an incident bremsstrahlung beam[9] obtained when an electron beam from a linear accelerator strikes a high-Z target such as gold. The incident "white" spectrum of the bremsstrahlung is modified by passing it through an absorber which generates narrow nuclear absorption dips in the outgoing spectrum. The particular shape and widths of these dips are determined by the lattice dynamics of the atoms of the solid absorber. Similarly, the nuclear levels of the scatterer, which contain the same nuclei as the absorber, are also Doppler broadened with widths

$$\Delta_i = E_\gamma (2kT_i/Mc^2)^{1/2}$$

($i = r,s$ correspond to scatterer and absorber), and their particular line shapes carry the lattice-dynamical information, which is of our concern here. When the artificially modified photon beam strikes a nuclear scatterer (containing the same nuclei as the absorber), the Doppler-broadened dips created by the absorber act as shape analyzers of the broadened levels. The overlap of the two shapes [shaded area in Fig. 1(d)] is proportional to the scattered intensity I_s. For an anisotropic solid, the effective temperature T_r is different in various directions, and hence I_s will depend on the orientation of the scatterer. It is important to point out that the anisotropy in the atomic motion of the solid depends primarily on the zero-point energies of the normal modes of motion of the atoms in the solid.[1] If the phonon spectrum of the system is known, it can be used for calculating the values of T_r in the different directions. The ratio of the scattering intensities corresponding to the different molecular orientations of the scatterer can then be evaluated and compared to experiment. In the case of the intercalated C_8K sample[5,6] this information may be used to test the phonon spectra of the K atoms along and perpendicular to the c axis of the target.

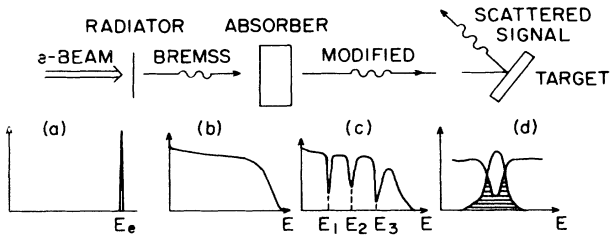

FIG. 1. Upper part describes from left to right the sequence of events in which (1) an electron beam strikes a high-Z radiator, (2) a bremsstrahlung beam is generated, (3) passes through a nuclear absorber, (4) scatters from a target. The lower diagrams represent schematic drawings of the spectra of (a) the monoenergetic electron beam, (b) the bremsstrahlung, (c) the bremsstrahlung shape after being modified by the absorber, (d) the shaded area illustrates the overlap integral between the incident shape of the "dip" and the Doppler-broadened shape of a resonant nuclear level.

III. THEORETICAL REMARKS

The calculation of the scattered intensities follows the method described in Ref. 10 for a white bremsstrahlung spectrum passing through a self-absorber and hitting a scatterer. In the present case both the self-absorber and the scatterers are thick requiring numerical integrations procedures. To get an intuitive understanding of the basic idea of the measurement, we note that for cases with $\Delta > \Gamma$, the scattered intensity I_s of the beam after passing through the nuclear absorber increases with Δ because a broader resonance results in smaller nuclear self-absorption. Since the effective temperature and hence Δ of a particular nuclear level in the sample depends on the sample orientation with respect to the photon beam one expects a dependence of I_s on the orientation. Furthermore, since the effective temperature increases with the binding forces, the magnitude of I_s from the ^{39}K nuclear levels can be viewed as a monitor of the strength of the directional forces binding the K atoms to the graphite basal planes. This point is illustrated in Fig. 2 which shows the calculated values of I_s from the 6.33 and the 5.26 MeV levels in ^{39}K as a function of the effective temperature of the scatterer. The widths and other parame-

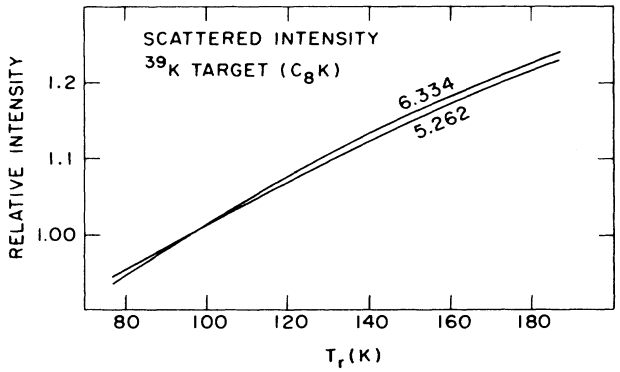

FIG. 2. Calculated scattering cross section from the 6.334 MeV ($g\Gamma_0^2/\Gamma = 2.0$ eV) and the 5.262 MeV ($g\Gamma_0^2/\Gamma = 0.55$ eV) levels in ^{39}K as a function of the effective temperature T_r of the scatterer. A bremsstrahlung beam modified by passing through a 7.9 g/cm^2 metallic K absorber before hitting a 10.6 g/cm^2 thick C_8K target is assumed. Cross sections are normalized to unity at $T_r = 95$ K.

ters necessary for carrying out this calculation were taken from Ref. 11. Figure 2 can also be used for calculating T_r in cases where the scattering cross section is known. In calculating I_s, one needs the effective temperatures of the metallic K absorber (T_e) and of that of the K scatterer along ($T_{||}$) and perpendicular ($T_\perp$) to the graphite planes of the C_8K target. The calculation is explained below.

A. Calculation of T_e for metallic K

The effective temperature T_e for metallic K can be calculated following Lamb[12] by assuming that metallic K conforms to the behavior of a Debye solid, whereby one obtains[12,13]

$$\frac{T_e}{T}=3\left[\frac{T}{\Theta_D}\right]^3\int_0^{\Theta_D/T}x^3\left[\frac{1}{e^x-1}+\frac{1}{2}\right]dx\ . \tag{1}$$

Using a Debye temperature $\Theta_D=91$ K for metallic K, the value of T_e versus T was calculated by employing Eq. (1) and is given in a graphic form in Fig. 3. It should be added that Eq. (1) seems to be applicable to metallic elements as was found to be the case for Pb and Ni where a critical study of T_e versus T was carried out using the NRPS method.[14] At very low temperatures, $T\rightarrow 0$ °K, T_e approaches a limiting value which gives an accurate measure of the zero-point energy of the K atoms in the C_8K lattice,

$$T_e=\tfrac{3}{8}\Theta_D\ . \tag{2}$$

In order to obtain the scattering cross sections along and perpendicular to the graphite planes, it is necessary to calculate the effective temperatures $T_{||}$ and $T_\perp$ along these two directions.

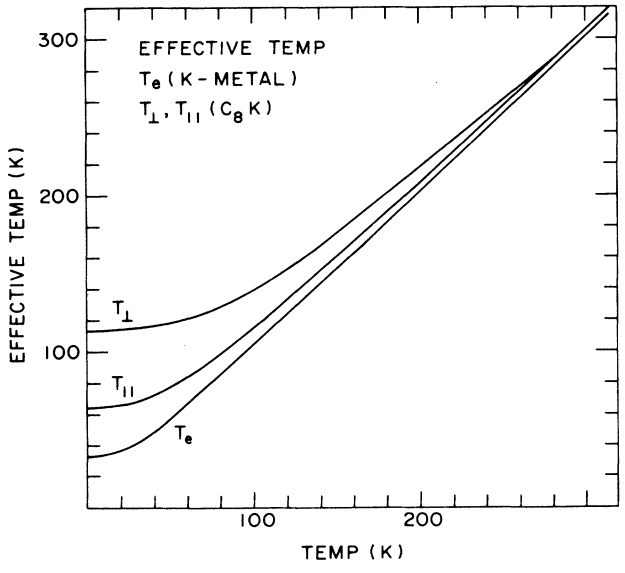

FIG. 3. Calculated effective temperatures versus T of the K atoms: T_e is for metallic K obtained using the Debye approximation [Eq. (1)]; $T_{||}$ and $T_\perp$, for K atoms in directions parallel and perpendicular to the graphite planes in the C_8K sample.

B. Calculation of $T_{||}$ of K

The effective temperature $T_{||}$ is related to the in-plane phonons of C_8K. The corresponding modes of vibrations were reported by Kamitakahara and Zabel,[6] using inelastic neutron scattering. To calculate $T_{||}$, we note that it should reflect the average energy of the K atom per mode of vibration (including the zero-point energy), thus

$$\varepsilon_{||}=kT_{||}=\frac{\int_0^{\nu_m}S_1(\nu)g_1(\nu)h\nu\alpha\,d\nu}{\int_0^{\nu_m}g_1(\nu)d\nu}\ . \tag{3}$$

$S_1(\nu)$ is the energy fraction[15] shared by the K atom in each vibrational mode.

$$\alpha=\{[\exp(h\nu/kT)-1]^{-1}+\tfrac{1}{2}\}=\tfrac{1}{2}\coth\frac{h\nu}{2kT}\ ,$$

and $g_1(\nu)$ is the phonon density of states of the in-plane modes of C_8K, with $\nu_m=\omega_m/2\pi$ the maximum phonon frequency occurring in the spectrum. An interesting point to note in this calculation is that the carbon atoms do not participate in those in-plane modes and are essentially decoupled from the higher energy graphite modes. Therefore, all the energy is carried by the K atoms, hence $S_1(\nu)=1$ in the above formula. In fact a small tail occurs in the spectrum which was ascribed to the graphite atoms and was subtracted. The above integration was carried out point by point numerically and evaluated as function of T. The results are given in Fig. 3 which at $T=78$ K yields $T_{||}=96.0$ K.

C. Calculation of $T_\perp$ of K

To calculate $T_\perp$ we used Eq. (3) with g_1 and S_1 replaced by $g_2(\nu)$ and $S_2(\nu)$. It is convenient to express g_2 in terms of q_r [the relative phonon wave vector $q_r=q(I_c/2\pi)$, with I_c the identity period] and to utilize the tabulated values of Zabel and Magerl[5] for the out-of-plane normal modes of C_8K,

$$g_2(\varepsilon)=\frac{dn}{dq_r}\frac{dq_r}{d\varepsilon}=2\frac{dq_r}{d\varepsilon}\ . \tag{4}$$

Thus $\varepsilon_\perp$ can be written in the form

$$\varepsilon_\perp=kT_\perp=2\int_0^{\varepsilon_m}\varepsilon S_2(\varepsilon)\frac{dq_r}{d\varepsilon}\alpha\,d\varepsilon\ , \tag{5}$$

where the integration interval is split into two separate regions covering the acoustical and optical branches. The energy fraction $S_2(\varepsilon)$ carried[15–18] by the K atoms in the out-of-plane vibrational modes is given by $S_2=E_k/(E_k+E_c)$ with E_k, E_c, and (E_k+E_c) the energies carried by the K plane, C plane, and the total energy of the phonon, respectively. For harmonic vibrational modes, S_2 can be expressed in terms of the amplitudes A_k and A_c,

$$S_2(\varepsilon)=M_kA_k^2/(M_kA_k^2+M_cA_c^2)\ , \tag{6}$$

with

$$E_k=\omega^2M_kA_k^2/2$$

and

$$E_c=\omega^2M_cA_c^2/2\ .$$

To calculate the amplitude ratio A_k/A_c, we used the same simple Born-von Karman model employed by Zabel and Magerl[5] which views the C_8K sample as composed of alternate rigid planes each consisting of either C atoms or K atoms with both the amplitudes of the motions and the wave vectors along the hexagonal c axis of the sample. Thus the [001] L dispersion is equivalent to that of a one-dimensional diatomic lattice in which the unit cell consists of two masses M_c, M_k in the ratio $M_c/M_k = 8\times 12{:}39 = 2.46{:}1$ having a force constant of $\phi = 4120$ dyn/cm with a repeat distance $I_c = 5.34$ Å. This simple model yields a value for A_k/A_c and substituting in the expression for S_2 above, one obtains

$$S_2(\varepsilon) = \left[1 + \frac{M_c}{M_k}[2\phi \cos\pi q_r/(2\phi - \varepsilon^2 M_c/h^2)]^2\right]^{-1} . \tag{7}$$

Using the values appearing in Table II of Ref. 5 for numerical integration of Eq. (3), we obtain $T_\perp$ versus T given in Fig. 3 which at $T = 78$ K yields $T_\perp = 128$ K. The calculated ratio $T_\perp/T_{||}$ which corresponds to a calculated cross-section ratio $\sigma_\perp/\sigma_{||} = 1.10$ is to be compared with the measured ratio as is done in Sec. V.

IV. EXPERIMENTAL METHOD

The bremsstrahlung photons were obtained from an electron beam at 8.5 MeV and 4 μA hitting a 196 mg/cm^2 gold radiator. The electrons were stopped by a 8.2 cm long (14.8 g/cm^2) graphite block placed in a Faraday cup which monitored the beam intensity. The electron beam was obtained from the MUSL-2 accelerator of the University of Illinois having a 100% duty cycle. The experimental system (Fig. 4) differed from that described in Ref. 19 only in the use of a 5 cm borated plastic shield (against fast neutrons) which greatly reduced the background. Two Ge(Li) detectors were used, at scattering angles of 90° and 127° each with a volume of 35 cm^3. Photon hardeners consisting of bismuth (14.9 g/cm^2), zinc (42.0 g/cm^2), and borated plastic (5.0 cm) were used at 90°, while at 127° the thicknesses were bismuth (14.8 g/cm^2), zinc (16.7 g/cm^2), and borated plastic (5.0 cm). The x-ray energy resolution of the system was $\sim$12 keV at 7 MeV. Other details of the experimental system, the electronics and data acquisition method are described elsewhere.[19]

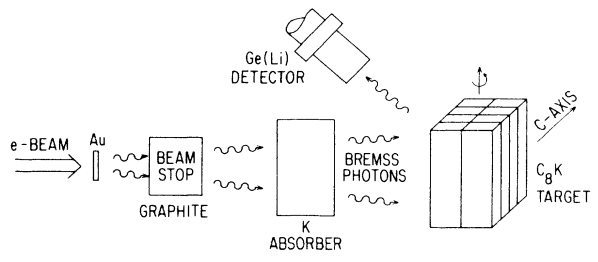

FIG. 4. Schematic arrangement (not to scale) showing the e beam, the gold radiator (Au), the graphite beam stop, the metallic K absorber, the oriented C_8K target (consisting of eight plates) and the detector. Both the K absorber and the C_8K target were kept at liquid-nitrogen temperature.

The target consisted of eight separated C_8K plates (Fig. 4) each with dimensions $73\times 21.5\times 8.7$ mm^3, oriented with its c axis perpendicular to the 73×21.5 mm^2 plane. (The eight plates were packed to form an orthorhombic shape of dimensions $73\times 43\times 35$ mm^3. Each plate was separately prepared using slabs of oriented pyrolytic graphite and employing the two-zone vapor transport method. The mosaic spread of the initial sample of pyrolytic graphite was $\Delta\eta \approx 7°$ and that of the C_8K sample after intercalation was $\eta \approx 12°$ at FWHM. The stage and homogeneity of each plate were determined by x-ray $(0,0,l)$ scans. The distance between adjacent graphite planes increases considerably (from 3.35 Å in pure graphite to 5.34 Å) upon intercalation. The target was coated with paraffin oil and covered with a very thin plastic foil to prevent oxidation. The beam was passed through a 7.9 g/cm^2 metallic K absorber sealed inside a lucite box before hitting the target. Both the target and the absorber were kept at liquid N_2 temperature by placing them inside styrofoam containers. In addition, the target container was placed on a rotatable table whose axis coincided with the long geometrical axis of the sample; it was repeatedly rotated by $+90°$ from a geometry where the photon beam was parallel to the c axis of the sample to a perpendicular geometry and vice versa.

V. RESULTS

The scattered radiation spectrum from a metallic K target sealed inside a lucite container is given in Fig. 5(a) which shows the various γ lines corresponding to nuclear resonance scattering from levels in ^{39}K and ^{12}C (present in the lucite container). Figure 5(b) shows the scattered spectrum from the cooled C_8K target obtained after passing the bremsstrahlung beam through a 7.9 g/cm^2 K absorber before hitting the target. The γ lines corresponding to resonance scattering from levels in ^{12}C and ^{14}N (arising from liquid N_2) and the strong nuclear absorption of some of the ^{39}K γ lines are clearly seen. The scattering intensities from the various levels in the two positions of the target were normalized to the total charge of the Faraday cup and corrected for counting rate losses. The cross-section ratios $\sigma_\perp/\sigma_{||}$ were then extracted after correcting for nuclear and atomic attenuation for the two target orientations. For the case of ^{39}K, the contribution from only two strongly excited levels of 6.334 and 5.263 MeV were taken into account and the measured value of $\sigma_\perp/\sigma_{||}$ given in Table I is an average over the above two levels. The table lists also the cross-section ratio for the 4.439 MeV, 2^+ level in ^{12}C which also yields anisotropic scattering effects, the reason being that the graphite block which stopped the electron beam also acts as a self-absorber thus generating an anisotropy in the scattered intensities from the ^{12}C present in the oriented C_8K sample. It is of interest to note that the scattered γ line at 7.03 MeV from ^{14}N revealed practically no anisotropy (Table I). This is expected because the ^{14}N was present in form of nonoriented liquid N_2, close to the C_8K sample. The fact that the ratio $\sigma_\perp/\sigma_{||}$ for ^{14}N is practically equal to unity, shows that our experimental system has essentially

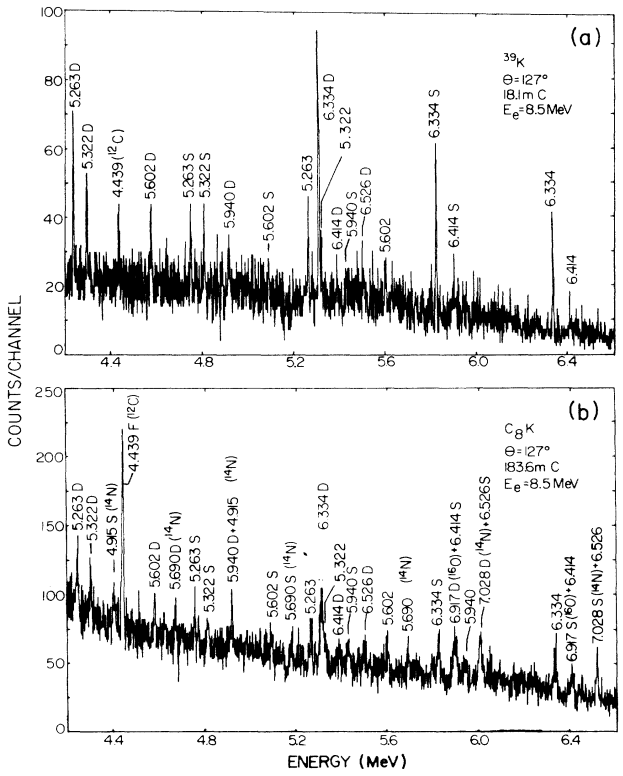

FIG. 5. (a) Scattered radiation spectrum from K target (inside a lucite container) obtained at 127° and 35 Ge(Li) detector using 8.5 MeV bremsstrahlung. (b) Scattered spectrum from a C_8K target (placed inside a styrofoam box containing liquid N_2). *S* and *D* refer to single- and double-escape peaks while other lines refer to the full-energy peaks of the various γ lines.

no spurious instrumental asymmetries which can arise from inaccuracies in the geometries of the incident bremsstrahlung beam with respect to the two orientations of the sample.

A. Anisotropy in the binding of the K atoms

In the present work, only the ratio of the scattered intensities has been measured and hence only the ratio of the effective temperatures can be extracted. Accepting the calculated value $T_{||}=96$ K at $T=78$ K to be correct, it is possible to deduce the value of $T_\perp$ from the measured ratio using Fig. 2. The result is

TABLE I. Measured scattering cross-section ratio from nuclear levels in ^{39}K, ^{12}C, and ^{14}N. The C_8K sample was cooled using liquid N_2 and was oriented with the photon beam perpendicular ($\sigma_\perp$) and parallel ($\sigma_{||}$) to the graphite planes.

Isotope	E_x (MeV)	$\sigma_\perp/\sigma_{||}$
^{39}K	6.33 + 5.26	1.16±0.06
^{14}N	7.028	1.04±0.06
^{12}C	4.44	0.88±0.06

$$T_\perp = 153 \pm 27 \text{ K} \quad \text{at } T = 78 \text{ K}$$

which marginally overlaps within one standard deviation the calculated value $T_\perp = 128$ K. The fact that the deduced value is markedly higher than the calculated one, could indicate that some of the high-frequency perpendicular modes contain an appreciable intercalant contribution not taken into account in the calculation of $T_\perp$ from the phonon dispersion of the low-lying longitudinal modes.

A consideration of Fig. 3 shows that the effective binding energy of the K atom parallel to the graphite surface is much stronger than the binding in metallic K. Furthermore the binding perpendicular to the *G* planes appears to be much stronger than that in the parallel direction. These differences are more pronounced at lower temperatures where the thermal motion is essentially frozen and the sole effect is due to the zero-point motion in the binding potential. In fact, in the vicinity of $T=20$ K, the ratio of the effective temperatures is seen to be $\frac{114}{66}=1.73$ as compared with $\frac{128}{96}=1.33$ at $T=78$ K. Thus, a study of the ratio $R=\sigma_\perp/\sigma_{||}$ as a function of T could yield more detailed information concerning the phonon spectrum. This, however, would require much longer running times using the electron linac, which are not available at present.

The binding of the K atoms in the two directions can also be expressed in terms of Debye temperatures in the limit of $T\to 0$ K using Eq. (2). For K atoms in C_8K, accepting $T_{||}=96$ K at $T=78$ K, one calculates from the phonon spectra the following values of Debye temperatures:

$$\Theta_{||}=173 \text{ K}, \quad \Theta_\perp=306 \text{ K}$$

for the directions parallel and perpendicular to the *G* planes. Further, our measured $\sigma_\perp/\sigma_{||}$ ratio yields

$$\Theta_{||}=173 \text{ K}, \quad \Theta_\perp=378\pm84 \text{ K}$$

to be compared with $\Theta_D=91$ K for metallic K. This shows again that the predominantly ionic forces governing the K-C interaction out-of-the plane and the K-K interaction in the plane are much stronger than the bonds of pure K in metallic form.

B. Anisotropy in the binding of the C atoms

It is of interest to consider the ratio of the scattered intensities from the 4.439 MeV level in ^{12}C occurring in the oriented C_8K target, and to try to find out to what extent this ratio can be reproduced if one accounts for the known anisotropic binding properties of the C atoms in the C_8K sample. In this case, no accurate calculation can be made because the 14.8 g/cm^2 graphite absorber which served to stop the electron beam is known to produce about 20% of the bremsstrahlung radiation hitting the C_8K target. Thus the effective thickness of the C absorber can be roughly estimated to be 13.6 g/cm^2. To calculate the anisotropy we used the following values for the effective temperatures of the C atoms.

(i) $T_e=685$ K for the nonoriented graphite absorber at room temperature ($T=295$ K).

(ii) $T_p=865$ K and $T_c=250$ K for the oriented C_8K

sample at $T=78$ K, in directions parallel and perpendicular to the graphite planes, respectively.

With these three temperatures, the calculated scattering cross-section ratio from the 4.439 MeV level in ^{12}C (having $g\Gamma_0^2/\Gamma=0.054$ eV) was found to be $\sigma_\perp/\sigma_{||}=0.90$ in good agreement with the experimental value (Table I). However, this estimate should be treated with some reservation because of all uncertainties and assumptions made as explained below. The value of T_e was calculated using Eq. (3) with $S_1(\nu)=1$ and employing the experimental phonon spectrum for graphite reported by Nicklow[20]. The values of T_c and T_p at $T=78$ K were calculated using Eq. (1) and employing the following Debye temperatures:[21,22] $\Theta_c=670$ K and $\Theta_p=2300$ K corresponding to the motion of the C atoms perpendicular and parallel to the graphite planes. Here we used the Debye temperatures of the C atoms for oriented graphite instead of that of the oriented C_8K target, thus we are assuming that the presence of the K atoms do not affect the high-frequency modes of the C atoms which are responsible for the high values of the Debye temperatures.

The fact that the above estimate of the anisotropy agrees with that obtained experimentally provides a self-consistency check of the whole procedure.

VI. DISCUSSION

As mentioned in Sec. I, the method of NRPS is capable of measuring the Debye temperature of individual nuclei, similar to the Mössbauer effect and more directly than in x-ray and neutron scattering experiments. To determine the Debye temperature on an absolute scale, one would need to measure the scattered intensities as a function of temperature, which was not possible in the present case. However, taking the ratio of the scattered intensities for two perpendicular sample orientations yields direct information on the ratio of the effective temperatures and ultimately on the ratio of the Debye temperatures for those two directions. Another important point to note is the fact that the experimental Debye temperatures determined via the Doppler broadening of the nuclear resonance levels are proportional to the mean-square velocity of the nuclei in question, and may thus deviate from Debye temperatures derived from mean-square displacements. On the other hand, the former method may provide valuable information on the participation of specific nuclei in high-frequency modes.

As mentioned in Sec. V A, the Debye temperatures for intercalated K obtained in the present work are $\Theta_{||}=173$ K and $\Theta_\perp=378\pm84$ K for the direction parallel and perpendicular to the graphite plane (G plane), respectively. Specific-heat measurements from Mizutani *et al.*[23] are not suitable for comparison, since they automatically take an orientational and a mass density average over all phonon modes. Leung *et al.*[24] measured the mean-square displacement $\langle z^2\rangle$ of the K layers parallel to the c axis via x-ray scattering. From their result of $\langle z^2\rangle=0.0416\pm0.0076$ Å^2 at room temperature we calculate a Debye temperature of $\Theta_\perp=475^{+55}_{-40}$ K, which overlaps the value $\Theta_\perp=378\pm84$ obtained in the present work. By comparing the two results one should keep in mind that the x-ray method requires four free parameters to fit the measured $(00l)$ Bragg intensities, which eventually results in the value of $\langle z^2\rangle$ needed for calculating $\Theta_\perp$.

As mentioned before, the Debye temperatures measured here are highly anisotropic with mean-square velocities being smaller, parallel than perpendicular to the intercalate plane. This is opposite to the behavior of the C atoms, which exhibit smaller vibrational velocities normal to the basal planes. This trend has already been noticed for the stage-1 C_8Cs compound by Campbell *et al.*,[25] who obtained from Mössbauer measurements $\Theta_{||}=76.5$ K and $\Theta_\perp=145$ K, respectively. In both cases C_8K and C_8Cs the anisotropy ratio $\Theta_\perp/\Theta_{||}$ is roughly a factor of two. Also, the Debye temperatures for the intercalated alkali atoms in both directions are considerably higher than those for the free alkali-metal atoms, which are 91 and 38 K for K and Cs, respectively. This indicates that the force constants for the alkali vibration normal to the intercalate planes are a factor of 12 to 14 larger than in the free alkali metals, in rough agreement with the ratio of the elastic constant $C_{33}^{G\text{-}K}/C_{11}^{K}=10.6$ and $C_{33}^{G\text{-}Cs}/C_{11}^{Cs}=24.5$, where C_{33} is the compressional elastic constant of the intercalated compounds normal to the layers[5] and $C_{11}^{K,Cs}$ is the corresponding elastic constant of pure K and Cs metals.[26,27] The stronger force constants in graphite are a consequence of the charge transfer from alkali atoms to the graphite planes resulting in an interplane metal-carbon interaction determined by a competition between Coulomb attraction and hard-core repulsion, and an alkali-alkali interaction determined almost entirely by the Coulomb interactions.[28]

Finally, the measured intensity ratio $\sigma_\perp/\sigma_{||}$ indicated a ratio of Debye temperatures which is larger than the one we calculated from the measured phonon dispersions. In the calculation we have taken only the low-lying phonon branches into account. According to the lattice-dynamical calculations by Horie *et al.*[29] and by Al-Jishi and Dreesselhaus[30] those are the modes with a significant alkali-intercalate contribution. However, since the NRPS method weights the contribution of each mode by the mean-square velocity rather than by the mean square displacement, it may be speculated that also higher-lying phonon modes, in particular the B_{1g} and A_{2u} modes at 560 cm^{-1}, contain some relevant alkali participation.

ACKNOWLEDGMENTS

This work was supported in part by the National Science Foundation under Grant No. NSF-PHY-83-11717 and also by the U.S. Department of Energy (Division of Materials Sciences), under Contract No. DE-AC02-76ER01198. One of us (R.M.) would like to acknowledge the support of the United States—Israel Binational Science Foundation (Jerusalem, Israel).

[1]O. Shahal and R. Moreh, Phys. Rev. Lett. **40**, 1714 (1978).
[2]R. Moreh, Phys. Lett. **107A**, 468 (1985).
[3]M. S. Dresselhaus and G. Dresselhaus, Adv. Phys. **30**, 139 (1981).
[4]S. A. Solin, Adv. Chem. Phys. **49**, 455 (1982).
[5]H. Zabel and Magerl, Phys. Rev. B **25**, 2463 (1982).
[6]W. A. Kamitakahara and H. Zabel, Phys. Rev. B **32**, 7817 (1985).
[7]R. Moreh and O. Shahal, Solid State Commun. **43**, 529 (1982).
[8]R. Moreh and O. Shahal, Phys. Rev. Lett. **43**, 1947 (1979).
[9]R. Moreh, W. C. Sellyey, and R. Vodhanel, Phys. Lett. **92B**, 286 (1980).
[10]H. W. Kuehne, P. Axel, and D. C. Sutton, Phys. Rev. **163**, 1278 (1967).
[11]R. Moreh, W. M. Sandefur, W. C. Sellyey, and D. C. Sutton (unpublished).
[12]W. E. Lamb, Phys. Rev. **55**, 190 (1939).
[13]F. R. Metzger, Prog. Nucl. Phys. **7**, 53 (1959).
[14]R. Moreh, O. Shahal, and I. Jacob, Nucl. Phys. A **228**, 77 (1974).
[15]R. Moreh, O. Shahal, and V. Volterra, Nucl. Phys. A **262**, 221 (1976).
[16]O. Shahal, R. Moreh, and M. Pazi, Nucl. Phys. A **339**, 157 (1980).
[17]R. Moreh, Nucl. Instrum. Methods **166**, 45 (1979).
[18]D. A. Neumann and H. Zabel, Phys. Rev. Lett. **53**, 56 (1984).
[19]T. Chapuran, R. Vodhanel, and M. K. Brussel, Phys. Rev. C **22**, 1420 (1980).
[20]N. Wakabayashi and R. M. Nicklow, in *Electrons and Phonons in Layered Crystal Structures*, edited by T. J. Wieting and M. Shluter (Reidel, Dordrecht, Holland, 1979), p. 409.
[21]A. Ludsteck, Acta Crystallogr. A **28**, 59 (1972).
[22]G. Albinet, J. P. Biberian, and M. Bienfait, Phys. Rev. B **3**, 2015 (1971).
[23]U. Mizutani, T. Kondow, and T. B. Massalski, Phys. Rev. B **17**, 3165 (1978).
[24]S. Y. Leung, M. S. Dresselhaus, C. Underhill, T. Krapchev, G. Dresselhaus, and B. J. Wuensch, Phys. Rev. B **24**, 3505 (1981).
[25]L. E. Campbell, G. L. Montet, and G. J. Perlow, Phys. Rev. B **15**, 3318 (1977).
[26]R. F. S. Hearmon, *Elastic, Piezoelectric and Related Constants of Crystals*, Vol. III/11 of *Landolt-Bornstein, New Series*, edited by K. H. Hellwege and A. M. Hellwege (Springer-Verlag, Berlin, 1979).
[27]F. J. Kollarits and J. Trivisonno, J. Phys. Chem. Solids **29**, 2133C (1968).
[28]D. P. DiVinceuzo and E. J. Mele, Phys. Rev. B **31**, 1136 (1985).
[29]C. Horie, M. Maeda, and Y. Kuramoto, Physica **99B**, 430 (1980).
[30]R. Al-Jishi and G. Dresselhaus, Phys. Rev. B **26**, 4523 (1982).